

Received January 2, 2020, accepted January 12, 2020, date of publication January 23, 2020, date of current version February 5, 2020.

Digital Object Identifier 10.1109/ACCESS.2020.2968956

Direction of Arrival Estimation and Robust Adaptive Beamforming With Unfolded Augmented Coprime Array

KUN ZHANG^{1,2}, (Member, IEEE), CHONG SHEN², (Member, IEEE), HANWEN LI³, ZHUANG LI⁴, HAIFENG WANG⁴, XIAOYAN CHEN⁴, AND JING CHEN⁴

¹Education Center of MTA, Hainan Tropical Ocean University, Sanya 572022, China

²State Key Laboratory of Marine Resource Utilization in South China Sea, Hainan University, Haikou 570228, China

³College of Ocean Information Engineering, Hainan Tropical Ocean University, Sanya 572022, China

⁴College of Computer Science and Technology, Hainan Tropical Ocean University, Sanya 572022, China

Corresponding author: Chong Shen (chongshen@hainanu.edu.cn)

This work was supported in part by the high-level talent project of Hainan Natural Science Foundation under Grant 2019RC236, in part by the National Natural Science Foundation of China under Grant 61861015, and in part by the Key Project of Scientific Research of Higher Education in Hainan Province under Grant HNKY2019ZD-35.

ABSTRACT An augmented coprime array systematically employs two sparse subarrays to produce a large-scale difference co-array with attractive merits, such as enhanced degrees of freedom (DOFs) and enlarged array aperture, whereas the interleaved subarrays are susceptible to mutual coupling. In this paper, we propose an unfolded augmented coprime array (UACA) obtained by careful crafting of small sparse subarrays to fill the holes in the difference co-array generated by unfolding operation. Specifically, UACA can significantly reduce the number of sensor pairs with small spacing and hence inherently weaken the mutual coupling effect. Meanwhile, an increase of the DOFs and improved direction of arrival (DOA) estimation accuracy can be achieved in the presence of mutual coupling. As an application of UACA, we propose a decoupled interference-plus-noise covariance matrix (INCM) reconstruction method for robust adaptive beamforming (RAB) with UACA. Therein, mutual coupling coefficients are estimated based on the remodeled contaminated steering vector and the noise subspace. The estimated mutual coupling matrix is utilized to reconstruct the decoupled covariance matrix which in turn is used to obtain refined DOA estimates, interferer power estimates, and the desired INCM. Extensive simulation results are provided to verify the effectiveness of UACA and the decoupled INCM reconstruction method for RAB.

INDEX TERMS Coprime array, mutual coupling, DOA estimation, robust adaptive beamforming.

I. INTRODUCTION

The small spacing between the adjacent antenna elements in traditional dense arrays is typically limited to half wavelength or less to avoid spatial aliasing, which leads to significant mutual coupling and restricted array aperture. In general, mutual coupling is intrinsically caused by complex electromagnetic interactions and is particularly severe for antenna pairs with small separation. In practice, mutual coupling can result in catastrophic performance degradation in the estimation of essential system parameters, such as complex channel gains [1] and directions of arrival (DOA) [2], [3]. To tackle

this problem, the minimum redundancy array (MRA) [4] was proposed to simultaneously obtain a sparse array structure which is less susceptible to mutual coupling, and to yield a large difference co-array with more antennas than the physical array for increased achievable degrees of freedom (DOFs). But a closed form expression for the sensor positions in MRA is not available, and it must be obtained through numerical search.

In recent years, two new non-uniform sparse arrays, namely the coprime array [5]–[14] and nested array [15]–[18], both with closed form position expressions for the physical array and difference co-array, have attracted much attention in the field of DOA estimation and beamforming, as they can lead to enhanced DOFs, enlarged array aperture and weakened

The associate editor coordinating the review of this manuscript and approving it for publication was Liangtian Wan¹.

mutual coupling. In particular, as indicated in [5], [6], [15], $O(T^2)$ DOFs can be obtained with only T antenna elements. The typical two-level nested array can generate a hole-free difference co-array, but incorporates one dense subarray with inter-element spacing of half wavelength, which results in undesired mutual coupling effect, as compared with coprime array and MRA. In [6], an augmented coprime array (ACA) was proposed which is composed of two sparse uniform linear subarrays with inter-element spacing of $N\lambda/2$ and $M\lambda/2$, where $2M$ and N are the number of sensors in the two subarrays ($N > M$), respectively, M and N are coprime integers, and λ denotes the operating wavelength. However, the two subarrays are interleaved and the resulting physical coprime array still suffers from mutual coupling. In contrast, in [12], [13], an unfolded coprime array (UCA) was proposed where the minimum adjacent distance between sensors is limited to multiple folds of half wavelength. In fact, the UCA can be regarded as a special case of a generalized coprime array, called CADiS [14], which introduces a displacement between the subarrays. Nevertheless, dispersed holes exist in the difference co-array generated by CADiS while optimization methods, *e.g.* sparse representation (SR) and compressed sensing (CS), are required to perform DOA estimation with the non-uniform co-array [19]–[23]. Alternatively, spatial smoothing technique and the Toeplitz method can be employed to obtain an effective semi-definite covariance matrix by selecting the consecutive parts in the difference co-array, where the two split consecutive co-arrays of CADiS will damage the achievable aperture and hence degrade the estimation performance. Subsequently, state-of-the-art approaches, such as MUSIC, ESPRIT, PM, and their variants can be applied to extract DOA estimates with the consecutive co-array. It is noteworthy that the methods based on SR and CS are also applicable to the consecutive co-array.

As one of the fundamental signal processing techniques, adaptive beamforming has been extensively used in various fields, such as radar, wireless communications and sonar, to acquire a desired signal and simultaneously reject interferers with a different spatial signature [24]–[28]. Specifically, the well-known Capon beamformer can offer distinguished resolution and the capability of interference suppression [29]. Nevertheless, it suffers from the model mismatch and performance degradation caused by look direction errors, limited number of samples and mutual coupling. In the past decades, various approaches have been introduced to enhance the beamformer robustness, *e.g.*, diagonal loading (DL) [30], eigenspace processing [31], [32], worst-case design [33] and interference covariance matrix reconstruction [34]. It is indicated in [34] that beamformers based on covariance matrix reconstruction can achieve remarkable output signal-to-interference-plus-noise ratio (SINR) performance, but are susceptible to mutual coupling effects. In [35], to address this issue, a novel adaptive beamforming method was proposed by utilizing the antenna elements to inherently suppress the mutual coupling. In [36], the mutual coupling coefficients were estimated by a subspace-based method,

allowing the calculation of a refined (compensated) beamforming weight vector. However, the aforementioned two methods are developed for the uniform linear array (ULA), which is characterized by limited DOFs and array aperture. Alternatively, in [37], a coprime array-based robust adaptive beamforming (RAB) technique was proposed wherein the covariance matrix is constructed by considering the difference co-array. Meanwhile, in [38], a related beamforming algorithm was proposed to achieve a trade-off between robustness and efficiency, whereby the coprime array is decomposed into two subarrays and hence the achievable DOFs are significantly reduced. Although the coprime array inherently leads to a reduction of the mutual coupling effect, these two approaches do not apply any compensation scheme, so that mutual coupling can still potentially degrade the beamformer performance.

In this paper, we firstly propose an unfolded augmented coprime array (UACA) obtained by careful crafting of small sparse subarrays to fill the holes in the difference co-array generated by the unfolding operation. As a result, UACA can significantly decrease the number of sensor pairs with small spacing, *i.e.* $d, 2d, \dots$, and hence inherently weaken the mutual coupling effect in the case $d = \lambda/2$. Meanwhile, an increase of the DOFs and improved DOA estimation performance can be achieved. Furthermore, as a potential application of UACA, we propose a decoupled interference-plus-noise covariance matrix (INCM) reconstruction method for RAB. By exploiting the improved DOA estimates and the associated total noise subspace, the mutual coupling coefficients are calculated based on the remodeled contaminated steering vectors. Subsequently, the estimated mutual coupling matrix is utilized to reconstruct the decoupled covariance matrix, which in turned is used to obtain refined DOA estimates, interferer power estimates, and the desired INCM. Extensive simulation results are provided to demonstrate the effectiveness of UACA and the decoupled INCM reconstruction method for RAB.

Specifically, the contributions of our work can be summarized as follows.

(a) We propose an extended coprime array, namely the UACA, where reduced mutual coupling, increased DOFs and enhanced spatial resolution are highly desirable. Specifically, we first unfold the interleaved subarrays in ACA to enlarge the array aperture and decrease the number of sensor pairs with small spacing, which are the main cause of the mutual coupling. We carefully design a small sparse subarray to fill the holes in the difference co-array of UCA, which leads to increased DOFs as compared with ACA and UCA.

(b) We derive closed form expressions for the physical locations of the UACA antennas and consecutive co-array and the DOFs. In addition, we prove that only one sensor pair in the UACA can produce a small separation of md for any integer $m \in \{1, 2, \dots, M-1\}$, except in the case of even M where one additional sensor pair exists with $Md/2$.

(c) We apply the proposed UACA to adaptive beamforming in the presence of mutual coupling. In addition to the

inherent capability of the UACA to suppress mutual coupling, we remodel the contaminated steering vector and estimate the mutual coupling matrix by exploiting the orthogonality between the signal and total noise subspaces.

(d) We use the estimated mutual coupling matrix to compensate for the contamination in the received signal and formulate a decoupled covariance matrix optimization to estimate the powers of the interferers. Finally, the refined INCM is utilized to construct the adaptive beamformer weight vector.

The rest of the paper is outlined as follows. In Section II, we provide some fundamental reviews of sparse array signal processing and RAB. In Section III, we introduce the proposed UACA and derive the closed-form expressions of the sensor locations in the UACA and associated subarrays and for the achievable DOFs. In Section IV, we present the decoupled INCM reconstruction method for RAB with UACA. In Section V, we provide numerical simulations to prove the effectiveness of UACA and the proposed INCM method for adaptive beamforming. Section VI finally concludes this paper.

Notations: We use upper-case (lower-case) bold characters to represent matrices (vectors). $(\cdot)^T$, $(\cdot)^*$ and $(\cdot)^H$, respectively, stand for the transpose, conjugation and conjugate transpose of a matrix or vector. $\text{diag}\{v\}$ generates a diagonal matrix which utilizes the vector v as its diagonal elements while $\text{diag}\{V\}$ takes the principal diagonal elements of matrix V to construct a diagonal matrix. $\langle a_1, a_2 \rangle$ denotes an integer set $\{a \in \mathbb{Z} | a_1 \leq a \leq a_2\}$ and $\mathbb{Z} = \{0, \pm 1, \dots\}$ is the set of integers. $\text{length}\{v\}$ represents the number of elements in vector v and $\lfloor a \rfloor$ rounds a to the nearest integer, where $\lfloor a \rfloor \leq a$. $E\{\cdot\}$ denotes the expectation operator and $\min\{\cdot\}$ is the minimization operator. $\text{vec}(A)$ is the vectorization operator to stack the columns of a matrix A and \circ denotes Khatri-Rao product. $\|\cdot\|_F$ denotes the Frobenius norm. $I_T \in \mathbb{R}^{T \times T}$ denotes the identity matrix with ones at the principal diagonal.

II. PRELIMINARIES

In this section, we briefly review sparse array signal processing and adaptive beamforming, as needed in the sequel.

A. DATA MODEL

Assume that K far-field incoherent and uncorrelated signals impinge on an array with T sensors and distribution set $\mathbb{S}_d = d\mathbb{S}$, where $d = \lambda/2$ is the unit spacing and $\mathbb{S} = \{d_j | d_j \in \mathbb{Z}, j = 1, 2, \dots, T\}$. The output of physical array can be expressed by

$$x(t) = As(t) + n(t), \quad t \in \langle 1, L \rangle \quad (1)$$

where $s(t) = [s_1(t), s_2(t), \dots, s_K(t)] \in \mathbb{C}^{K \times 1}$ is the signal vector, $n(t) \in \mathbb{C}^{T \times 1}$ is the white Gaussian noise with mean zero and variance σ_n^2 which is independent of the signals and L represents the number of snapshots. $A = [a(\theta_1), a(\theta_2), \dots, a(\theta_K)] \in \mathbb{C}^{T \times K}$ denotes the directional

matrix with columns, *i.e.* steering vectors, is defined by

$$a(\theta_k) = [e^{-j\pi d_1 \sin \theta_k}, e^{-j\pi d_2 \sin \theta_k}, \dots, e^{-j\pi d_T \sin \theta_k}]^T \quad (2)$$

where θ_k is the azimuth angle of the k -th signal ($k = 1, 2, \dots, K$).

The covariance matrix of the received signal is defined by

$$R_x = E \left\{ x(t)x^H(t) \right\} = AR_sA^H + \sigma_n^2 I_T \quad (3)$$

where the signal covariance matrix is defined by $R_s = E \left\{ s(t)s^H(t) \right\} = \text{diag} \left\{ \sigma_1^2, \sigma_2^2, \dots, \sigma_K^2 \right\}$ and σ_k^2 stands for the power of the k -th signal. $I_T \in \mathbb{R}^{T \times T}$ denotes the identity matrix with ones at the principal diagonal. In practice, the covariance matrix R_x is calculated with finite number of snapshots by

$$\hat{R}_x = \frac{1}{L} \sum_{t=1}^L x(t)x^H(t) \quad (4)$$

Definition 1: (co-arrays). For a given physical array with distribution set $\mathbb{S}_d = d\mathbb{S}$, the difference co-array \mathbb{D}_d and consecutive co-array \mathbb{U}_d are defined by

$$\begin{aligned} \mathbb{D}_d &= d\mathbb{D} = \{(d_i - d_j)d \mid d_i, d_j \in \mathbb{S}\} \\ \mathbb{U}_d &= d\mathbb{U} = d \langle D_1, D_2 \rangle \subseteq \mathbb{D}_d \end{aligned} \quad (5)$$

where \mathbb{U} contains the largest number of continuous integers in \mathbb{D} and is specified by D_1, D_2 . Then the consecutive DOF (cDOF) is given by $\text{cDOF} = D_2 - D_1 + 1$. Note that the difference co-array can possess more than one consecutive co-array, whereas the cDOF remains constant.

Definition 2: (weight function). For a physical array with distribution set $\mathbb{S}_d = d\mathbb{S}$, the weight function $w(l)$ denotes the number of sensor pairs producing the l -th virtual sensor in the difference co-array

$$\begin{aligned} \mathbb{M}(l) &= \{(n_1, n_2) \mid n_1 - n_2 = l \in \mathbb{D}; n_1, n_2 \in \mathbb{S}\} \\ w(l) &= \text{length}\{\mathbb{M}(l)\} \end{aligned} \quad (6)$$

where $\mathbb{M}(l)$ incorporates all the sensor pairs producing the l -th virtual sensor.

According to [15], the difference and consecutive co-array can be obtained by vectorizing the covariance matrix as

$$v = \text{vec}(R_x) = (A^* \circ A)\eta + \sigma_n^2 \text{vec}(I_T) \quad (7)$$

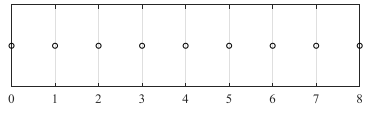
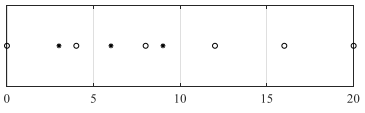
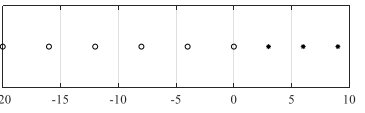
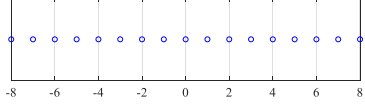
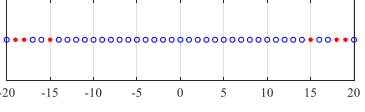
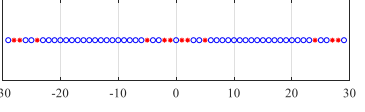
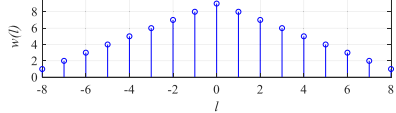
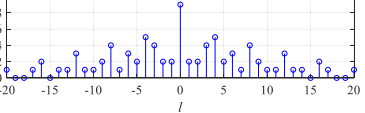
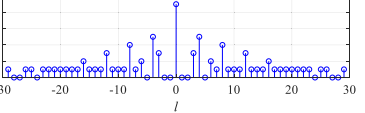
where $\eta = [\sigma_1^2, \sigma_2^2, \dots, \sigma_K^2]^T$. By reshaping v , we can obtain the equivalent received signal of the difference co-array [15].

B. ROBUST ADAPTIVE BEAMFORMING

In this part, we define $s_1(t)$ as the desired signal and the other $K - 1$ signals as interferers. Then the array output can be represented by

$$\begin{aligned} x(t) &= d(t) + i(t) + n(t) \\ &= a(\theta_1)s_1(t) + A_i s_i(t) + n(t) \end{aligned} \quad (8)$$

TABLE 1. ULA, ACA and UCA.

	ULA	ACA	UCA
\mathbb{S}			
\mathbb{D}			
$w(t)$			
L_C	0.7682	0.5953	0

where $d(t) = a(\theta_1)s_1(t)$ is the desired signal vector, $i(t) = A_i s_i(t)$ represents the interference vector and $A_i = [a(\theta_2), \dots, a(\theta_K)] \in \mathbb{C}^{T \times (K-1)}$.

The output of a beamformer is given by

$$y(t) = w^H x(t) \tag{9}$$

where $w \in \mathbb{C}^{T \times 1}$ is the corresponding weight vector. The SINR of the array output is employed to evaluate the beamformer performance and is defined by

$$\text{SINR} = \frac{\sigma_1^2 |w^H a(\theta_1)|^2}{w^H R_{i+n} w} \tag{10}$$

where the INCM R_{i+n} is given by

$$\begin{aligned} R_{i+n} &= E \left\{ [i(t) + n(t)][i(t) + n(t)]^H \right\} \\ &= \sum_{k=2}^K \sigma_k^2 a(\theta_k) a^H(\theta_k) + \sigma_n^2 I_T \end{aligned} \tag{11}$$

The MVDR beamformer can be constructed by solving the following minimization problem

$$\min_w w^H R_{i+n} w \text{ subject to } w^H a(\theta_1) = 1 \tag{12}$$

where the solution is given by [29]

$$w = \frac{R_{i+n}^{-1} a(\theta_1)}{a^H(\theta_1) R_{i+n}^{-1} a(\theta_1)} \tag{13}$$

In practice, R_{i+n} is usually unavailable and is substituted by the estimated covariance matrix \hat{R}_x

$$w_{\text{SMI}} = \frac{\hat{R}_x^{-1} a(\theta_1)}{a^H(\theta_1) \hat{R}_x^{-1} a(\theta_1)} \tag{14}$$

where w_{SMI} is the sample matrix inversion (SMI) beamformer [39].

C. MUTUAL COUPLING

According to [35], [36], [40]–[42], the mutual coupling coefficient between the adjacent sensors is inversely proportional to the inter-element spacing and it can be neglected in the case of the sensor pair with a few folds of half wavelength. Specifically, a B -banded model of mutual coupling for ULA is defined as

$$[C]_{p,q} = \begin{cases} 0 & |d_p - d_q| \geq B \\ c_{|d_p - d_q|} & |d_p - d_q| < B \end{cases} \tag{15}$$

where $[C]_{p,q}$ denotes the element in C for the p -th row and q -th column and $d_p, d_q \in \mathbb{S}$. B represents the threshold of mutual coupling, i.e., the mutual coupling can be ignored when the inter-element spacing is larger than Bd . In the presence of mutual coupling, the array output in (1) needs modifying as

$$\tilde{x}(t) = CAs(t) + n(t) \tag{16}$$

where $C \in \mathbb{C}^{T \times T}$. Additionally, the coupling leakage is employed to measure the intensity of mutual coupling and is defined by [16]

$$L_C = \frac{\|C - \text{diag}\{C\}\|_F}{\|C\|_F} \tag{17}$$

where $\|\cdot\|_F$ denotes the Frobenius norm.

III. UNFOLDED AUGMENTED COPRIME ARRAY

In this section, we first review the ACA and UCA to give the motivation of this paper. Subsequently, we introduce the proposed UACA and offer the closed form expressions of the physical UACA, consecutive co-array and achievable cDOFs.

A. REVIEW

As illustrated in [6], ACA is composed of two interleaved subarrays with $2M$ and N sensors ($N > M$), where the distances of adjacent sensors are Nd and Md , respectively. One example of ACA is exhibited in the second column of

Table 1 along with the difference co-array, weight function and coupling leakage, where $M = 3, N = 4$ and $B = 3, c_0 = 1, c_1 = 0.9e^{-j\pi/3}, c_2 = 0.75e^{j\pi/4}$ [36]. It is shown clearly that multiple sensor pairs are involved in the physical ACA with high coupling leakage of 0.5953. In [12], [13], the two interleaved subarrays are unfolded and UCA is proposed to suppress the mutual coupling. In the third column of Table 1, an example of UCA is provided, where $M = 3, N = 4$. In particular, we make a replication of subarray with $M = 3$ sensors in UCA to better illustrate the relation between UCA and ACA, where the concept of unfolding is still straightforward. Specifically, according to Table 1, UCA possesses no sensor pair with separation of md ($m \in \langle 1, 2 \rangle$), which effectively eliminate the sensitivity against mutual coupling. However, according to the second row, the difference co-array of UCA has scattered holes, which crucially harms the consecutive co-array and hence the achievable cDOFs.

B. UNFOLDED AUGMENTED COPRIME ARRAY

Definition 3 (Unfolded Augmented Coprime Array): UACA consists of three subarrays with $2M, N$ and $\lfloor M/2 \rfloor$ sensors, respectively, where M, N are coprime integers and $M < N$. The total number of sensors in UACA is $T = N + 2M - 1 + \lfloor M/2 \rfloor$. The distance between adjacent sensors in the subarray with N sensors is $d_{s1} = Md$ and the other two subarrays have $d_{s2} = Nd$, where $d = \lambda/2$ and λ is the wavelength. Specifically, the distribution set $\mathbb{S}_d = d\mathbb{S}$ of UACA is provided

$$\begin{cases} \mathbb{S}_1 = \langle 0, (N - 1) \rangle M \\ \mathbb{S}_2 = \langle -(2M - 1), 0 \rangle N \\ \mathbb{S}_3 = \langle 1, \lfloor M/2 \rfloor \rangle N \\ \mathbb{S} = \mathbb{S}_1 \cup \mathbb{S}_2 \cup \mathbb{S}_3 \end{cases} \quad (18)$$

Property of UACA:

- (a) The consecutive co-array of UACA is specified by $\langle -D_a, D_a \rangle$, where $D_a = 2MN + M - 1$ and $\text{cDOF} = 2D_a + 1$.
- (b) Weight function.

For odd $M, w(l) = 1$ when $l \in \langle 1, M - 1 \rangle$.

$$\text{For even } M, w(l) = \begin{cases} 1, & l \in \langle 1, M - 1 \rangle \ \& \ l \neq M/2 \\ 2, & l = M/2 \end{cases}$$

Illustratively, we give a prototype of UACA in Table 2 along with the difference co-array and weight function, where $M = 3, N = 4$ and the mutual coupling coefficients are the same as Table 1 with $B = 3$. As shown in the first row of TABLE 2, UACA can be configured by assembling UCA and a small subarray with $\lfloor M/2 \rfloor = 1$ sensor, where resultantly, only one sensor is interleaved with the subarray with $N = 4$ sensors. According to the weight function of UACA in the third row of Table 2, only one sensor pair with separation of md ($m \in \langle 1, 2 \rangle$) is involved in the physical array, which means the resulting UACA can inherently reduce the mutual coupling and in this case, the coupling leakage of UACA is $0.4641 < 0.5953$. In addition, finite number of mutual coupling coefficients are inserted in the B -banded mutual

TABLE 2. UACA.

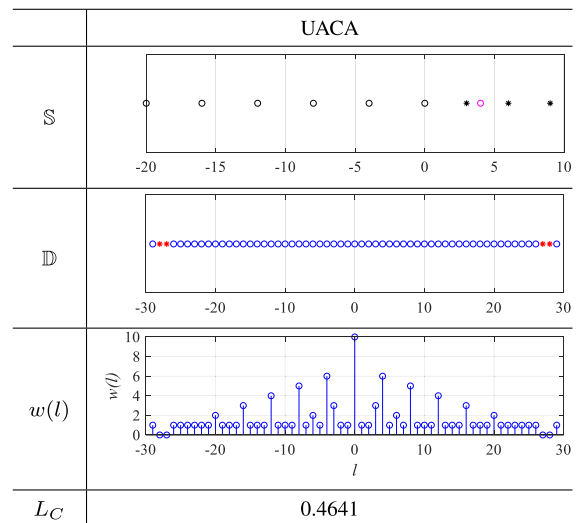


TABLE 3. Decoupled INCM Reconstruction Method for RAB with UACA.

<i>Input:</i> Received signal of UACA $\tilde{x}(t), t \in \langle 1, L \rangle$
<i>Output:</i> Beamformer weight for UACA w_{UACA}
1. compute \tilde{R}_x according to (19);
2. obtain \tilde{v}_c by vectorizing \tilde{R}_x ;
3. construct \tilde{R}_v as (21) and calculate $\hat{\theta}_k^{\text{ini}}$ ($k \in \langle 1, K \rangle$);
4. construct P and calculate E_n ;
5. construct $Z(\theta)$ and calculate \hat{c} ;
6. calculate \tilde{R}_d to obtain $\hat{\theta}_k^r$ ($k \in \langle 1, K \rangle$);
7. compute \hat{R}_s via (32) and \hat{R}_{i+n} via (35);
8. calculate w_{UACA} with \hat{R}_{i+n} and $a(\hat{\theta}_1^r)$.

coupling model. Furthermore, in the second row of Table 3, the holes in the central part of difference co-array generated by UCA are filled by the small subarray with $\lfloor M/2 \rfloor = 1$ sensor, which contributes to the increase of achievable cDOFs of UACA, as compared with ACA and UCA.

C. DISCUSSION

The proposed UACA utilizes an additional sparse subarray with $\lfloor M/2 \rfloor$ sensors to fill the central holes in the difference co-array of UCA and hence can obtain a significant increase of DOFs. In Fig. 2, we provide the cDOF comparison of coprime arrays, *i.e.* UACA, ACA and UCA, where we set $N = M + 1$. As UACA incorporates an extra subarray with $\lfloor M/2 \rfloor$ sensors, we concatenate the small subarray with the $2M$ -sensor subarray in the ACA and UCA for fair comparison, where we give an example of ACA and UCA, respectively, in Fig. 1 with $M = 3, N = 4$. It is clearly shown from Fig. 2 that UACA has an advantage over ACA and UCA in cDOF especially with large number of total sensors. In addition, we provide the coupling leakage results in Fig. 3, where the mutual coupling coefficients are the

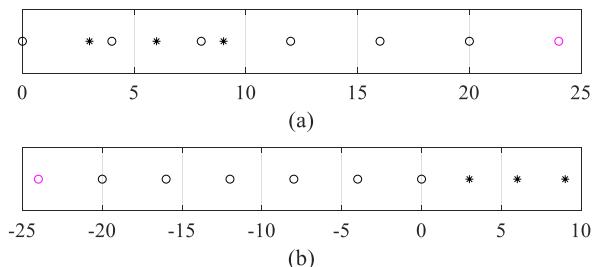


FIGURE 1. Considered ACA and UCA, where $M = 3, N = 4$. (a) ACA. (b) UCA.

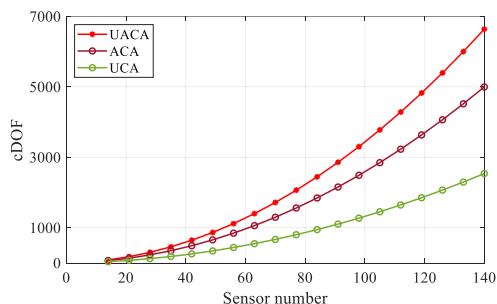


FIGURE 2. CDOF comparison of coprime arrays, where $N = M + 1$.

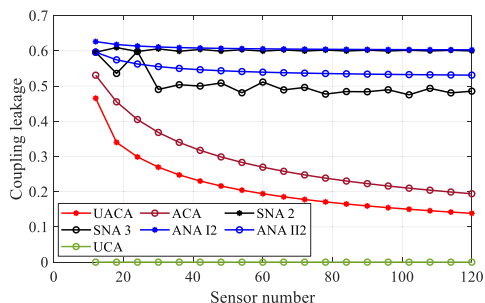


FIGURE 3. Coupling leakage comparison of different array, where $N = M + 1$.

same as Table 1 with $B = 3$, which verifies that UACA takes weaker mutual coupling effect than ACA and the nested arrays which are constructed according to [43], [44]. In the simulation part, the merits of UACA, *i.e.* the enhanced array aperture and mitigated mutual coupling, both contribute to the improved DOA estimation performance.

IV. ROBUST ADAPTIVE BEAMFORMING WITH UACA

In this section, we first calculate the initial DOA estimates by utilizing the contaminated output in (16) and constructing a semi-definite covariance matrix by Toeplitz technique. Then the mutual coupling coefficients are estimated based on the initial DOA estimates and the orthogonal relation between the remodeled steering vector and the total noise subspace. Finally, a decoupled covariance matrix is constructed based on the estimated mutual coupling matrix to obtain refined DOA estimates and power estimates of the interferers.

A. INITIAL DOA ESTIMATION

As shown in Table 2, UACA offers a large array aperture due to the sparse arrangement and is inherently less susceptible to mutual coupling. Consequently, we can directly employ the output in (16) to obtain the well performed DOA estimates.

Assume that UACA is constructed as *Definition 3*, where three subarrays have $2M, N$ and $\lfloor M/2 \rfloor$ sensors, respectively. The total number of sensors in UACA is $T = N + 2M - 1 + \lfloor M/2 \rfloor$. According to (4), the contaminated covariance matrix can be calculated by

$$\tilde{R}_x = \frac{1}{L} \sum_{t=1}^L \tilde{x}(t)\tilde{x}^H(t) \tag{19}$$

Then we reshape \tilde{R}_x via vectorization as [6], [15]

$$\tilde{v} = \text{vec}(\tilde{R}_x) \tag{20}$$

The equivalent observation vector $\tilde{v}_c \in \mathbb{C}^{(2D_a+1) \times 1}$ of the consecutive co-array by UACA can be obtained by selecting the rows from \tilde{v} corresponding to the distribution set \mathbb{U}_d . Instead of performing spatial smoothing technique with additional complex multiplications, we directly construct a semi-definite covariance matrix based on Toeplitz technique as [45]

$$\tilde{R}_v = \begin{bmatrix} \tilde{v}_c(D_a + 1) & \tilde{v}_c(2) & \cdots & \tilde{v}_c(1) \\ \tilde{v}_c(D_a + 2) & \tilde{v}_c(D_a + 1) & \cdots & \tilde{v}_c(2) \\ \vdots & \vdots & \ddots & \vdots \\ \tilde{v}_c(2D_a + 1) & \tilde{v}_c(2D_a) & \cdots & \tilde{v}_c(D_a + 1) \end{bmatrix} \tag{21}$$

where $D_a = 2MN + M - 1$ is provided in *Definition 3*. As proved in [45], \tilde{R}_v is equivalent to the spatial smoothing covariance matrix and MUSIC spectra are identical by exploiting \tilde{R}_v and the spatial smoothing covariance matrix if the noise and signal subspaces are specified by eigenvalues. The initial well-performed DOA estimates, denoted by $\hat{\theta}_k^{ini}$ ($k \in \{1, K\}$), can be directly obtained by searching the peaks of MUSIC spectra which are experimentally verified by numerical simulations in Section V.

B. MUTUAL COUPLING COEFFICIENTS ESTIMATION

In this subsection, we use the initial DOA estimates to calculate the mutual coupling coefficients.

To begin with, in the following derivation, we assume that $B = M$ for simplification, which is unnecessary in practical circumstances. The contaminated steering vector can be rewritten by

$$\begin{aligned} \tilde{a}_p(\theta) &= P\tilde{a}(\theta) \\ &= A_p(\theta)u(c, \theta) \end{aligned} \tag{22}$$

where P is the permutation matrix which is dependent on the inter-element spacing relation within the array structure,

c contains the mutual coupling coefficients and

$$A_p(\theta) = \begin{bmatrix} a_f(\theta) & & & & \\ & a_{b_1}(\theta) & & & \\ & & \ddots & & \\ & & & & a_{b_{J+1}+1}(\theta) \end{bmatrix} \quad (23)$$

$$u(c, \theta) = \begin{bmatrix} 1 \\ 1 + c_{b_1} \beta^{d_{b_1+1} - d_{b_1}} \\ c_{b_2-1} \beta^{d_{b_2-1} - d_{b_2}} + 1 + c_{b_2} \beta^{d_{b_2+1} - d_{b_2}} \\ \vdots \\ c_{b_J} \beta^{d_{b_J} - d_{b_J+1}} + 1 \end{bmatrix} \quad (24)$$

where $a_f(\theta) \in \mathbb{C}^{F \times 1}$ is a sub-vector of $\tilde{a}(\theta)$ corresponding to the F uncontaminated elements and $d_{b_j} \in \mathbb{S}$, $\beta = e^{-j\pi \sin \theta}$.

According to the orthogonal relation between the signal and noise subspace, we can get

$$\tilde{a}^H(\theta) E_n E_n^H \tilde{a}(\theta) = 0 \quad (25)$$

where E_n is the noise subspace of \tilde{R}_x . By multiplying the permutation matrix P , (25) can be transformed into

$$\begin{aligned} & \tilde{a}_p^H(\theta) (P^{-1})^H E_n E_n^H P^{-1} \tilde{a}_p(\theta) \\ &= u^H(c, \theta) A_p^H(\theta) (P^{-1})^H E_n E_n^H P^{-1} A_p(\theta) u(c, \theta) \\ &= u^H(c, \theta) Z(\theta) u(c, \theta) = 0 \end{aligned} \quad (26)$$

where

$$Z(\theta) = A_p^H(\theta) (P^{-1})^H E_n E_n^H P^{-1} A_p(\theta) \quad (27)$$

According to [36], based on the DOA estimates $\hat{\theta}_k^{ini}$ ($k \in \langle 1, K \rangle$) in Section IV.A, the estimate of $u(c, \hat{\theta}_k^{ini})$ is related to the eigenvector of the smallest eigenvalue of $Z(\hat{\theta}_k^{ini})$, represented by ζ . With the constraint $[u(c, \hat{\theta}_k^{ini})]_1 = 1$, we can obtain $\hat{u}(c, \hat{\theta}_k^{ini})$ by

$$\hat{u}(c, \hat{\theta}_k^{ini}) = \zeta \quad \text{subject to } [\zeta]_1 = 1 \quad (28)$$

where $[\zeta]_1$ stands for the first element of ζ .

Furthermore, we can directly calculate \hat{c} based on (a.9) in Appendix B and then construct the estimated mutual coupling matrix \hat{C} . As the available number of mutual coupling coefficients is limited in the mutual coupling matrix of UACA, \hat{c} relies on accurate DOA estimates. Resultantly, in this paper, we employ the estimated DOA with maximum MUSIC spectrum peak to calculate the mutual coupling coefficients.

As we have obtained \hat{C} , we can mitigate the mutual coupling effect by

$$\begin{aligned} \tilde{x}_d(t) &= \hat{C}^{-1} \tilde{x}(t) \\ &\approx d(t) + i(t) + \hat{C}^{-1} n(t) \\ &= a(\theta_1) s_1(t) + A_i s_i(t) + \hat{C}^{-1} n(t) \end{aligned} \quad (29)$$

In practice, we can directly calculate the decoupled covariance matrix by

$$\tilde{R}_d = \hat{C}^{-1} \tilde{R}_x (\hat{C}^H)^{-1} \quad (30)$$

where refined DOA estimates can be obtained based on \tilde{R}_d , denoted by $\hat{\Theta}^r = [\hat{\theta}_1^r, \hat{\theta}_2^r, \dots, \hat{\theta}_K^r]$.

C. POWER ESTIMATION OF INTERFERERS

Up to now, the decoupled covariance matrix and refined DOA estimates are obtained which are utilized to estimate the powers of desired signal and interferers.

Different from the joint covariance matrix optimization in [38] which dismisses the cross correlation of subarrays and neglects the mutual coupling effect, we formulate the decoupled covariance matrix optimization with \tilde{R}_d as [46]

$$\min_{R_s} \left\| \tilde{R}_d - A(\hat{\Theta}^r) R_s A^H(\hat{\Theta}^r) - \hat{\sigma}_n^2 I_T \right\|_F^2 \quad \text{subject to } R_s \geq 0 \quad (31)$$

where $\hat{\sigma}_n^2$ is the power estimate of noise which can be approximately computed by averaging the minimum $T - K$ eigenvalues of \tilde{R}_x . Moreover, the solution to the inequality-constrained optimization problem in (31) is given by

$$\begin{aligned} \hat{R}_s &= \text{diag} \left\{ \left[A_v^H A_v \right]^{-1} A_v^H r \right\} \\ &= \text{diag} \left\{ [\hat{\sigma}_1^2, \hat{\sigma}_2^2, \dots, \hat{\sigma}_K^2]^T \right\} \end{aligned} \quad (32)$$

where

$$A_v = \left[\text{vec} \left(a(\hat{\theta}_1^r) a^H(\hat{\theta}_1^r) \right), \dots, \text{vec} \left(a(\hat{\theta}_K^r) a^H(\hat{\theta}_K^r) \right) \right] \quad (33)$$

$$r = \text{vec} \left(\tilde{R}_d - \hat{\sigma}_n^2 I_T \right) \quad (34)$$

Subsequently, the INCM can be computed by

$$\hat{R}_{i+n} = \sum_{k=2}^K \hat{\sigma}_k^2 a(\hat{\theta}_k^r) a^H(\hat{\theta}_k^r) + \hat{\sigma}_n^2 I_T \quad (35)$$

According to the MVDR principal, the beamformer weight for UACA can be constructed by

$$w_{\text{UACA}} = \frac{\hat{R}_{i+n}^{-1} a(\hat{\theta}_1^r)}{a^H(\hat{\theta}_1^r) \hat{R}_{i+n}^{-1} a(\hat{\theta}_1^r)} \quad (36)$$

In addition, we summarize the detailed steps of the proposed decoupled INCM reconstruction method for RAB with UACA in Table 3.

V. NUMERICAL SIMULATIONS

In this section, we assume that a 17-sensor UACA is employed with $M = 5$ and $N = 6$. In Table 4, we calculate the coupling leakage and cDOFs for the corresponding configurations. Firstly, we give the root mean square error (RMSE) results to evaluate the DOA estimation performance

TABLE 4. Coupling leakage and cDOF of different configurations.

	UACA	ACA	SNA 2
L_C	0.2005	0.2572	0.2770
cDOF	129	93	161
	SNA 3	ANA I2	ANA II2
L_C	0.2770	0.2849	0.2689
cDOF	161	173	193

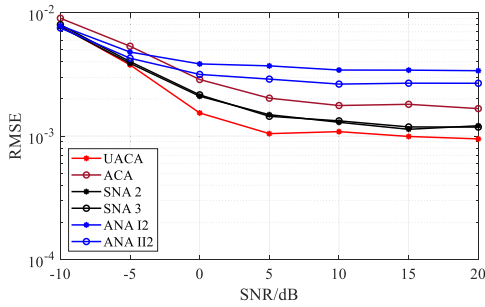


FIGURE 4. RMSE results of considered arrays versus SNR, where $T = 17$, $K = 17$ and $L = 500$.

with UACA via Toeplitz-MUSIC algorithm [45]. RMSE is defined by

$$RMSE = \sqrt{\frac{1}{200K} \left(\sum_{q=1}^{200} \sum_{k=1}^K (\delta_k - \hat{\delta}_{k,q})^2 \right)} \quad (37)$$

where $\delta_k = (\sin \theta_k)/2$ is the theoretical normalized DOA of the k -th signal and the estimate for the q -th trial is represented as $\hat{\delta}_{k,q} = (\sin \hat{\theta}_{k,q})/2$. Subsequently, we assess the proposed method for RAB with UACA, where the array output SINR results, defined by (10), are exhibited.

A. RMSE PERFORMANCE

In this simulation, we exhibit the RMSE results of Toeplitz-MUSIC algorithm with UACA, ACA and nested arrays, where $\delta_k = -0.2 + 0.4 \times (k - 1)/16$, $k \in \langle 1, 17 \rangle$, $K = 17$ and the search step is 0.001. In particular, we adopt the mutual coupling coefficients defined in [16]–[18] to provide the RMSE results for fair comparison, where $c_0 = 1$, $c_1 = 0.4e^{j\pi/3}$, $c_n = c_1 e^{-j(n-1)\pi/8}/n$ ($n \in \langle 2, B - 1 \rangle$) and $B = 100$. In Fig. 4, the proposed UACA can obtain the superior DOA estimation performance to other configurations via Toeplitz-MUSIC algorithm, where $L = 500$. It is revealed that UACA can remarkably mitigate the mutual coupling even with less cDOFs than nested arrays which suffer from redundant sensor pairs with small inter-element spacing. It is noteworthy that super nested arrays (SNAs), *i.e.* SNA 2 and SNA 3, outperform the augmented nested arrays (ANAs), namely ANA I2 and ANA II2, with reduced cDOFs, which shows that ANAs are sensitive to strong mutual coupling in the case of each sensor contaminated by the mutual coupling

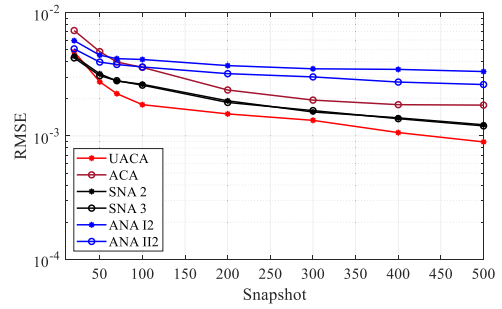


FIGURE 5. RMSE results of considered arrays versus snapshot, where $T = 17$, $K = 17$ and $SNR = 20$ dB.

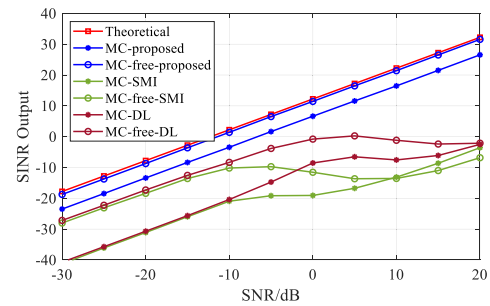


FIGURE 6. SINR output of three beamformer versus input SNR, where $L = 100$.

effect. Furthermore, in Fig. 5, the RMSE results versus number of snapshots are given, where $SNR = 20$ dB. It depicts that the RMSE performance of Toeplitz-MUSIC algorithm with UACA improves and takes advantages over that with the other configurations.

B. SINR OUTPUT

In this simulation, we assume that one desired signal with $\theta_1 = 10^\circ$ and two interferers with $\theta_2 = -20^\circ$ and $\theta_3 = 40^\circ$ impinge on UACA with $M = 5$ and $N = 6$, where the interference-to-noise ratio (INR) is set to $INR = 30$ dB, $B = 5$ and $c_0 = 1$, $c_1 = 0.9e^{-j\pi/3}$, $c_2 = 0.75e^{j\pi/4}$, $c_3 = 0.45e^{-j\pi/10}$, $c_4 = 0.15e^{-j\pi/6}$ [36]. The SMI beamformer [39] and DL beamformer [30] are employed to measure the proposed method, where the DL factor is set to $10\hat{\sigma}_n^2$. In Fig. 6, the SINR outputs versus input SNR of three beamformers with UACA are exhibited in the scenario of exactly known desired signal, where the prefix of MC in the figure means that the beamformer is directly constructed by the contaminated received signal while MC-free is to utilize the decoupled received signal with the estimated mutual coupling matrix. It is shown obviously that the three beamformers all achieve SINR output enhancement because the mutual coupling effect is alleviated by the utilization of the estimated mutual coupling matrix. SMI beamformer encounters performance degradation when SNR is larger than -5 dB as in this case, the output covariance matrix is contaminated by the desired signal component. The proposed beamformer outperforms the other two beamformers because the INCM

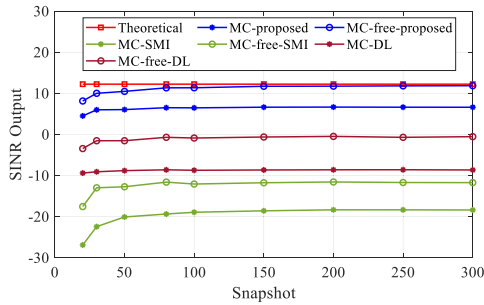


FIGURE 7. SINR output of three beamformer versus input snapshot, where SNR = 0dB.

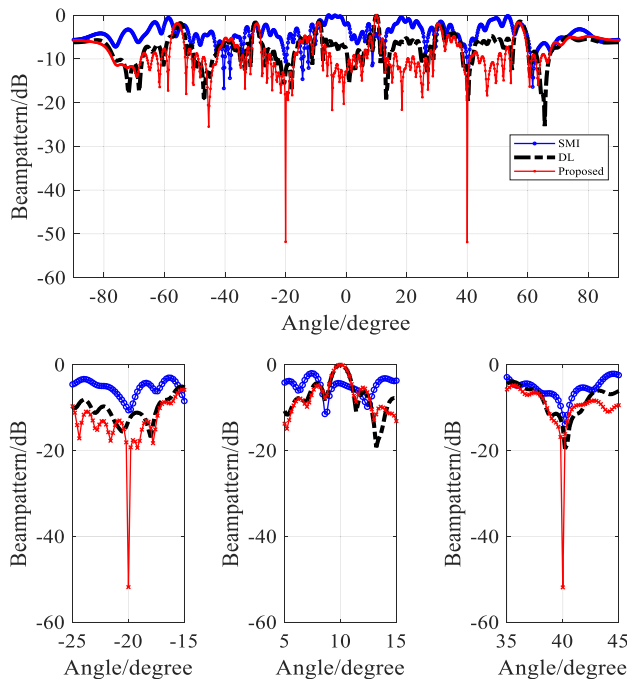


FIGURE 8. Beampatterns of three beamformers and the zoom-in figures, where SNR = 5dB, INR = 30dB and L = 100.

is reconstructed with well performed estimates of DOAs and powers of the interferers, where the desired signal component is considerably rejected in INCM. Moreover, as UACA can inherently alleviate the mutual coupling effect, the proposed beamformer obtained by the contaminated received signal is superior to the other two beamformers even with the aid of the estimated mutual coupling. Furthermore, the SINR output of the proposed beamformer is very close to the theoretical SINR output when the decoupled received signal is employed. In addition, the SINR outputs of the three beamformers versus snapshots are captured in Fig. 7, where SNR = 0dB, and we can also conclude that the proposed beamformer gains superior performance with the estimated mutual coupling matrix.

C. BEAMPATTERNS

In this part, we depict the beampatterns of the three beamformers with decoupled received signal in Fig. 8 and zoom-in

figures for better illustration, where input SNR = 5dB, INR = 30dB and L = 100. It is shown clearly that the proposed beamformer outperforms the other two beamformers, where the nulls and mainlobe can accurately target to the interferer and the desired signal. SMI beamformer gets the worst performance due to the contamination of output covariance matrix by the desired signal. Furthermore, although the DL beamformer can have the similar mainlobe to the proposed beamformer, it fails to null the interferer with $\theta_2 = -20^\circ$. In addition, the proposed beamformer can suppress the interferers with the deepest nulls at $\theta_2 = -20^\circ$ and $\theta_3 = 40^\circ$.

VI. CONCLUSION

In this paper, we propose the UACA by unfolding the interleaved subarrays of ACA and elaborately designing a small sparse subarray to fill the holes in difference co-array generated by unfolding operation. As a result, UACA can significantly decrease the number of sensor pairs with small spacing and hence inherently alleviate the mutual coupling effect. Simultaneously, an increase of DOFs and improved DOA estimation performance can be achieved which are both attractive in massive MIMO systems. In addition, we apply UACA to RAB and propose a decoupled INCM reconstruction method. By exploiting the initial DOA estimates obtained from the contaminated output, the mutual coupling matrix is estimated to construct the decoupled covariance matrix, where the refined DOA estimates can be obtained. Furthermore, a decoupled covariance matrix optimization is proposed to estimate the powers of interferers and then obtain the decoupled INCM. Extensive simulation results corroborate the effectiveness of UACA and the decoupled INCM reconstruction method.

REFERENCES

- [1] X. Wang, L. Wan, M. Huang, C. Shen, and K. Zhang, "Polarization channel estimation for circular and non-circular signals in massive MIMO systems," *IEEE J. Sel. Topics Signal Process.*, vol. 13, no. 5, pp. 1001–1016, Sep. 2019.
- [2] H. Wang, L. Wan, M. Dong, K. Ota, and X. Wang, "Assistant vehicle localization based on three collaborative base stations via SBL-based robust DOA estimation," *IEEE Internet Things J.*, vol. 6, no. 3, pp. 5766–5777, Jun. 2019.
- [3] X. Wang, L. Wang, X. Li, and G. Bi, "Nuclear norm minimization framework for DOA estimation in MIMO radar," *Signal Process.*, vol. 135, pp. 147–152, Jun. 2017.
- [4] A. Moffet, "Minimum-redundancy linear arrays," *IEEE Trans. Antennas Propag.*, vol. 16, no. 2, pp. 172–175, Mar. 1968.
- [5] P. P. Vaidyanathan and P. Pal, "Sparse sensing with co-prime samplers and arrays," *IEEE Trans. Signal Process.*, vol. 59, no. 2, pp. 573–586, Feb. 2011.
- [6] P. Pal and P. Vaidyanathan, "Coprime sampling and the MUSIC algorithm," in *Proc. IEEE Digit. Signal Process. Workshop IEEE Signal Process. Educ. Workshop*, Sedona, AZ, USA, Jan. 2011, pp. 289–294.
- [7] P. P. Vaidyanathan and P. Pal, "Theory of sparse coprime sensing in multiple dimensions," *IEEE Trans. Signal Process.*, vol. 59, no. 8, pp. 3592–3608, Aug. 2011.
- [8] C. Zhou, Z. Shi, Y. Gu, and X. Shen, "DECOM: DOA estimation with combined MUSIC for coprime array," in *Proc. IEEE Int. Conf. Wireless Commun. Signal Process.*, Hangzhou, China, Oct. 2013, pp. 1–5.
- [9] C. Zhou, Y. Gu, X. Fan, Z. Shi, G. Mao, and Y. D. Zhang, "Direction-of-arrival estimation for coprime array via virtual array interpolation," *IEEE Trans. Signal Process.*, vol. 66, no. 22, pp. 5956–5971, Nov. 2018.

- [10] C. Zhou, Y. Gu, Z. Shi, and Y. D. Zhang, "Off-grid direction-of-arrival estimation using coprime array interpolation," *IEEE Signal Process. Lett.*, vol. 25, no. 11, pp. 1710–1714, Nov. 2018.
- [11] W. Zheng, X. Zhang, and H. Zhai, "Generalized coprime planar array geometry for 2-D DOA estimation," *IEEE Commun. Lett.*, vol. 21, no. 5, pp. 1075–1078, May 2017.
- [12] J. Li and X. Zhang, "Direction of arrival estimation of quasi-stationary signals using unfolded coprime array," *IEEE Access*, vol. 5, no. 99, pp. 6538–6545, 2017.
- [13] W. Zheng, X. Zhang, P. Gong, and H. Zhai, "DOA estimation for coprime linear arrays: An ambiguity-free method involving full DOFs," *IEEE Commun. Lett.*, vol. 22, no. 3, pp. 562–565, Mar. 2018.
- [14] S. Qin, Y. D. Zhang, and M. G. Amin, "Generalized coprime array configurations for direction-of-arrival estimation," *IEEE Trans. Signal Process.*, vol. 63, no. 6, pp. 1377–1390, Mar. 2015.
- [15] P. Pal and P. P. Vaidyanathan, "Nested arrays: A novel approach to array processing with enhanced degrees of freedom," *IEEE Trans. Signal Process.*, vol. 58, no. 8, pp. 4167–4181, Aug. 2010.
- [16] C.-L. Liu and P. P. Vaidyanathan, "Super nested arrays: Linear sparse arrays with reduced mutual coupling—Part I: Fundamentals," *IEEE Trans. Signal Process.*, vol. 64, no. 15, pp. 3997–4012, Aug. 2016.
- [17] C.-L. Liu and P. P. Vaidyanathan, "Super nested arrays: Linear sparse arrays with reduced mutual coupling—Part II: High-order extensions," *IEEE Trans. Signal Process.*, vol. 64, no. 16, pp. 4203–4217, Aug. 2016.
- [18] J. Liu, Y. Zhang, Y. Lu, S. Ren, and S. Cao, "Augmented nested arrays with enhanced DOF and reduced mutual coupling," *IEEE Trans. Signal Process.*, vol. 65, no. 21, pp. 5549–5563, Nov. 2017.
- [19] J. Shi, G. Hu, X. Zhang, F. Sun, and H. Zhou, "Sparsity-based two-dimensional DOA estimation for coprime array: From sum-difference coarray viewpoint," *IEEE Trans. Signal Process.*, vol. 65, no. 21, pp. 5591–5604, Nov. 2017.
- [20] D. Malioutov, M. Cetin, and A. Willsky, "A sparse signal reconstruction perspective for source localization with sensor arrays," *IEEE Trans. Signal Process.*, vol. 53, no. 8, pp. 3010–3022, Aug. 2005.
- [21] P. Pal and P. Vaidyanathan, "Correlation-aware techniques for sparse support recovery," in *Proc. IEEE Statistical Signal Process. Workshop*, Ann Arbor, MI, USA, Aug. 2012, pp. 289–294.
- [22] C. Zhou, Z. Shi, Y. Gu, and N. Goodman, "DOA estimation by covariance matrix sparse reconstruction of coprime array," in *Proc. IEEE Int. Conf. Acoust., Speech Signal Process.*, Brisbane, QLD, Australia, Apr. 2015, pp. 2369–2373.
- [23] F. Sun, Q. Wu, Y. Sun, G. Ding, and P. Lan, "An iterative approach for sparse direction-of-arrival estimation in co-prime arrays with off-grid targets," *Digit. Signal Process.*, vol. 61, pp. 35–42, Feb. 2017.
- [24] C. Zhou, Y. Gu, W. Song, Y. Xie, and Z. Shi, "Robust adaptive beamforming based on DOA support using decomposed coprime subarrays," in *Proc. IEEE ICASSP*, Shanghai, China, Mar. 2016, pp. 2986–2990.
- [25] L. Wan, L. Sun, X. Kong, Y. Yuan, K. Sun, and F. Xia, "Task-driven resource assignment in mobile edge computing exploiting evolutionary computation," *IEEE Wireless Commun.*, vol. 26, no. 6, pp. 94–101, Dec. 2019.
- [26] Q. Shi, L. Liu, W. Xu, and R. Zhang, "Joint transmit beamforming and receive power splitting for MISO SWIPT systems," *IEEE Trans. Wireless Commun.*, vol. 13, no. 6, pp. 3269–3280, Jun. 2014.
- [27] R. Pec and Y. S. Cho, "Receive beamforming techniques for an LTE-based mobile relay station with a uniform linear array," *IEEE Trans. Veh. Technol.*, vol. 64, no. 7, pp. 3299–3304, Jul. 2015.
- [28] B. Liao, K. M. Tsui, and S. C. Chan, "Robust beamforming with magnitude response constraints using iterative second-order cone programming," *IEEE Trans. Antennas Propag.*, vol. 59, no. 9, pp. 3477–3482, Sep. 2011.
- [29] J. Capon, "High-resolution frequency-wavenumber spectrum analysis," *Proc. IEEE*, vol. 57, no. 8, pp. 1408–1418, Aug. 1969.
- [30] H. Cox, R. M. Zeskind, and M. M. Owen, "Robust adaptive beamforming," *IEEE Trans. Acoust., Speech Signal Process.*, vol. ASSP-35, no. 10, pp. 1365–1376, Oct. 1987.
- [31] L. Chang and C.-C. Yeh, "Performance of DMI and eigenspace-based beamformers," *IEEE Trans. Antennas Propag.*, vol. 40, no. 11, pp. 1336–1347, Nov. 1992.
- [32] D. Feldman and L. Griffiths, "A projection approach for robust adaptive beamforming," *IEEE Trans. Signal Process.*, vol. 42, no. 4, pp. 867–876, Apr. 1994.
- [33] S. Vorobyov, A. Gershman, and Z.-Q. Luo, "Robust adaptive beamforming using worst-case performance optimization: A solution to the signal mismatch problem," *IEEE Trans. Signal Process.*, vol. 51, no. 2, pp. 313–324, Feb. 2003.
- [34] Y. Gu and A. Leshem, "Robust adaptive beamforming based on interference covariance matrix reconstruction and steering vector estimation," *IEEE Trans. Signal Process.*, vol. 60, no. 7, pp. 3881–3885, Jul. 2012.
- [35] Z. Ye and C. Liu, "Non-sensitive adaptive beamforming against mutual coupling," *IET Signal Process.*, vol. 3, no. 1, pp. 1–6, 2009.
- [36] Z. Zheng, K. Liu, W.-Q. Wang, Y. Yang, and J. Yang, "Robust adaptive beamforming against mutual coupling based on mutual coupling coefficients estimation," *IEEE Trans. Veh. Technol.*, vol. 66, no. 10, pp. 9124–9133, Oct. 2017.
- [37] K. Liu and Y. D. Zhang, "Coprime array-based robust beamforming using covariance matrix reconstruction technique," *IET Commun.*, vol. 12, no. 17, pp. 2206–2212, Oct. 2018.
- [38] C. Zhou, Y. Gu, S. He, and Z. Shi, "A robust and efficient algorithm for coprime array adaptive beamforming," *IEEE Trans. Veh. Technol.*, vol. 67, no. 2, pp. 1099–1112, Feb. 2018.
- [39] H. V. Trees, *Optimum Array Processing*. New York, NY, USA: Wiley, 2002.
- [40] B. Friedlander and A. Weiss, "Direction finding in the presence of mutual coupling," *IEEE Trans. Antennas Propag.*, vol. 39, no. 3, pp. 273–284, Mar. 1991.
- [41] T. Svantesson, "Mutual coupling compensation using subspace fitting," in *Proc. IEEE Sensor Array Multichannel Signal Process. Workshop*, Cambridge, MA, USA, Mar. 2000, pp. 494–498.
- [42] T. Svantesson, "Direction finding in the presence of mutual coupling," M.S. thesis, Dept. Signals Syst., School Elect. Comput. Eng., Chalmers Univ. Technol., Chalmers, Sweden, 1999.
- [43] C. Liu, *Super Nested Arrays (1D)*. Accessed: Aug. 8, 2017. [Online]. Available: <http://systems.caltech.edu/dsp/students/clliu/SuperNested.html>
- [44] J. Liu, *Augmented Nested Arrays*. Accessed: Jul. 22, 2017. [Online]. Available: <http://www.mathworks.com/matlabcentral/fileexchange/57648-augmented-nested-array>
- [45] C.-L. Liu and P. P. Vaidyanathan, "Remarks on the spatial smoothing step in coarray MUSIC," *IEEE Signal Process. Lett.*, vol. 22, no. 9, pp. 1438–1442, Sep. 2015.
- [46] Y. Gu, N. A. Goodman, S. Hong, and Y. Li, "Robust adaptive beamforming based on interference covariance matrix sparse reconstruction," *Signal Process.*, vol. 96, pp. 375–381, Mar. 2014.

• • •